JOURNAL OF MATERIALS SCIENCE, 30 (1995) 4761–4769

Matrix morphology and fibre pull-out strength of T700/PPS and T700/PET thermoplastic composites

LIN YE*
Centre for Advanced Materials Technology, Department of Mechanical and Mechatronic Engineering, The University of Sydney, NSW 2006, Australia

T. SCHEURING, K. FRIEDRICH
Institute for Composite Materials Ltd., University of Kaiserslautern, 67663 Kaiserslautern, Germany

The main objective of this fundamental study was to investigate effects of processing conditions and resulting matrix morphology on interfacial bond strength of fibre reinforced thermoplastic composites. Using a hot stage microscope, single fibre pull-out samples were produced with T700S high strength carbon fibre and two semicrystalline thermoplastic matrices, polyphenylene sulphide (PPS) and polyethylene terephthalate (PET), respectively. Processing temperatures and cooling histories were the major variables in sample preparation. The T700S fibre had no clear effect on the surrounding PPS and PET matrix morphology, as long as direct cooling at constant rates was selected. A transcrystalline phase around the fibres could be induced in the T700S/PPS system, if isothermal crystallization was carried out at 227 °C. Fibre pull-out tests were conducted at room temperature and two basic failure paths were observed, i.e. debonding at the fibre–matrix interface and cohesive failure of the matrix close to the fibre surface. The results indicate that slow cooling rate and a resulting coarse spherulitic morphology around the fibres correlate with high interfacial shear strength. In fact somewhat higher strength values were obtained for samples with transcrystalline layers around the fibres.

1. Introduction

A critical issue of semicrystalline thermoplastic composites is the high dependency of the microstructure or morphology of the matrix material on the processing parameters [1–7]. Morphological aspects such as degree of crystallinity, spherulite size, lamella thickness and crystalline orientation have a profound effect on the ultimate properties of the polymer matrix. This situation gets complicated further by the effect of the reinforcing fibres on the morphology of the matrix. The nature of the fibre–matrix interface in composites, in general but most specifically in thermoplastic systems, remains one of the most technologically important but least understood aspects in composite materials' design. It was suggested, for instance, that the reason for the good fibre–matrix adhesion in carbon fibre/PEEK (APC-2) composites is based on the tendency of the fibres to generate transcrystallinity [8]. The nucleation of a transcrystalline region around the reinforcing fibres is thought to be central to the improvement of some composite properties [9–11]. Effects of transcrystallinity on composite properties are still unclear, however, and some results in this area are somewhat contradictory [12–14].

In composites, the effects of matrix morphology around fibres (e.g. transcrystallinity) on mechanical properties and fibre–matrix interfacial bond strength can be very complicated. Furthermore, the mechanisms by which transcrystallinity occurs are not fully understood. In particular, no method exists by which its appearance in a particular fibre–matrix combination can be predicted. The fibre material and surface energy, topology and surface coating, thermal conductivity, the matrix type and extensional flow during processing, and thermal history have all been reported to affect transcrystallinity in thermoplastic composites to some extent [15–17]. The various phenomena make an interpretation of interfacial bond strength data under the occurrence of a transcrystalline interphase rather difficult. In addition, the general testing methods, which do not distinctively isolate the major contributing aspects, exacerbate the controversy in the open literature. Many techniques have been devised to assess interface properties. From the methods currently available for characterization of the interfacial bond strength of model fibrous composite systems [18], the single fibre pull-out test [19–20] is probably one of the best suited for this purpose, because the method is potentially advantageous in

*Author to whom correspondence should be addressed.

0022–2461

TABLE I Basic properties of T700S carbon fibres

Density	($g\,cm^{-3}$)	1.80
Tensile strength	(MPa)	4800
Young's modulus	(GPa)	230
Elongation to break	(%)	2.1
Diameter	(μm)	7–8
Mass per unit length	(Tex)	800

in-situ observation of the matrix morphology and failure process at the interface.

In this study, attempts have been made to investigate and evaluate the effects of matrix morphology around the fibres (with or without transcrystalline interphase) on the fibre–matrix interfacial bond strength. Using T700S high strength carbon fibres with polyphenylene sulphide (PPS) and polyethylene terephthalate (PET) semicrystalline thermoplastic matrices, two model composite systems were studied.

2. Materials and specimen preparation

2.1. Fibres

The carbon fibre, used in this study, was T700S high strength carbon fibre [21]. The exact description of the fibre yarn is "T700S 12K C", where "C" refers to a non-twisted yarn with a special sizing to keep the 12 000 filaments together. Basic properties of the T700 carbon fibres are listed in Table I. In order to select a single carbon filament, the sizing was removed by immersing the fibre bundle in a methylethylketone (MEK) solution for 24 h, then washing it with fresh MEK in an ultrasonic cleaner for 30 min. This procedure was repeated once again and then the fibre tow was dried in an oven at 80 °C for 2 h. Now a single fibre could easily be separated from the bundle with the help of a magnifying glass and a white padding.

2.2. Matrices

Polyphenylene sulphide (PPS) used in this study was fine powder (Ryton®). PPS is a high performance thermoplastic with excellent chemical and physical properties [22] and a potential matrix for advanced composite materials. PPS polymer is normally highly crystalline in its basic and annealed form. The melting temperature, T_m, of PPS is 285 °C.

Polyethylene terephthalate (PET) was taken from a 65: 35 wt% glass fibre/PET comingled fabric. PET is an engineering plastic widely used in applications, associated with high modulus, good tensile strength and excellent chemical resistance. The degree of crystallinity of PET polymer varies with the processing history. The melting point of PET polymer is 265 °C [23].

2.3. Sample preparation

Standard fresh glass slides and cover glasses were used as basic elements for the preparation of single fibre pull-out samples (Fig. 1). Preliminary experiments revealed that the maximum embedded length of the

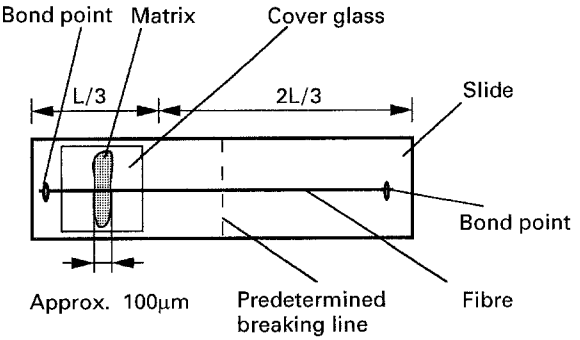

Figure 1 Preparation of a fibre pull-out sample based on a single fibre and polymer filament.

T700 carbon fibre in the matrix is about 100 μm for PET and 150 μm for PPS in order to successfully pull out the fibre in the tests. To get such tiny matrix filaments, different methods for PET and PPS polymers were applied.

From the "as received" PPS powder, filaments were spun from the molten PPS with a soldering iron. The filaments had a diameter between 15 and 40 μm, which gave a desired embedded length when the filaments melt again. Twisted PET bundles of three to five filaments were separated directly from the glass fibre/PET comingled fabric, consequently a desired embedded length was achieved.

A thermal system FP 900 with a FP 90 central processor and a FP 82 hot stage was used, for the sample production, associated with a Leitz Laborlux 12 Pol S optical microscope with crossed polaroids and a video camera. Temperature range of the hot stage could be controlled very accurately between room temperature and 375 °C. In addition, computer generated images could be obtained via the video camera using a MD30-IM PLUS image analysis software package.

The single fibre pull-out specimens were prepared by first sticking a single T700 carbon fibre onto two ends of the glass slide using a fast bond adhesive and placing the polymer filament(s) over it. Covered with a standard cover glass, the slide was put into the hot stage. On reaching the melting point of the polymer matrix, the molten polymer filament(s) wetted around the carbon fibre, being pressed by the weight of the cover glass. In this manner, fibre pull-out specimens of various embedded fibre lengths were obtained. Before the sample was put into the hot stage, one fibre end was removed from the bond point on the opposite side of the polymer filament. In this way fracture of the fibre could be avoided, in case the slide cracked during thermal processing cycles in the hot stage. It was confirmed after each pull-out test that the carbon fibres in specimens prepared this way were fully wrapped with polymer matrix.

The slide consisting of the single T700 fibre and the polymer filament(s) was subjected to a temperature regime. The T700/PPS specimens were rapidly heated at a heating rate of 20 °C min^{-1} from room temperature to 320 °C and held at this temperature for 2 min (holding time). Afterwards the samples were cooled down to 30 °C with three different cooling rates of

20 °C min^{-1}, 3 °C min^{-1} and 1 °C min^{-1}, respectively. To get a transcrystalline layer around the fibre, a special cooling history was chosen. The specimens were first cooled down to 227 °C at a cooling rate of 20 °C min^{-1} and held there isothermally for 10 min. They were then further cooled down to 30 °C at the same cooling rate. The temperature of 227 °C is equivalent to the melt crystallization temperature, T_{mc}, which was determined from cooling curves of the PPS polymer in the temperature range 220–240 °C, depending on the molecular weight and morphological structure [22].

The T700/PET specimens were prepared using a similar procedure described for the T700/PPS; however, transcrystallinity was not investigated. The specimens were rapidly heated to 300 °C, held for a period of 2 min, and then cooled down to 30 °C with cooling rates of 20 °C min^{-1} and 5 °C min^{-1}, respectively.

3. Experimental procedure

A tensile appliance (Minimat) was used for the single fibre pull-out tests. All experiments were conducted at room temperature with a constant cross-head speed of 0.5 mm min^{-1}. The experimental process was fully controlled using a computer unit with which the load-displacement flow charts could be recorded. Figs 2 and 3 illustrate schematically the testing fixture and the specimen holders with a sample.

In those pull-out tests in which the embedded fibre length was too long, the load rose linearly with increasing cross-head displacement, and reached a maximum point when the carbon fibre broke under tension. The breaking loads amounted to 120 mN in most cases, which agrees with the tensile strength of T700S carbon fibres. Conversely, if the embedded fibre lengths were appropriate, the fibres were pulled out from the matrix without breaking under tension. Under the movement of the cross-head, the load increased steadily up to the occurrence of an instantaneous load drop-off owing to debonding at the fibre–matrix interface and/or cohesive shear failure of the matrix. This was followed by a serrated load versus displacement trace, indicating the frictional pull-out of the fibre [24], as shown in Fig. 4.

The critical loads before the sudden drop-off, denoted as F_c, were measured for the two fibre–matrix systems with a variety of embedded fibre lengths. Then the apparent interfacial shear strength τ_{ic} was calculated using the following equation

$$\tau_{ic} = \frac{F_c}{\pi d L} \quad (1)$$

where d is the fibre diameter, and L the embedded fibre length [20], which was determined during the sample production in the hot stage using the connected image analyser.

4. Results and discussion

4.1. Matrix morphology

The semicrystalline PPS crystallizes very rapidly near the exothermic crystallization peak T_c, as observed during thermal analysis of a quenched sample [22]. In this study, a broad spectrum of spherulite sizes was observed for the PPS polymer subjected to different thermal processing cycles. For example, the average spherulite size amounted to 60 μm for a cooling rate of 20 °C min^{-1} but to 200 μm for 1 °C min^{-1}. In addition, the spherulite size is dependent on the processing temperature (T_p) prior to cooling and the dwell time in which the melt is held at this temperature. The higher the processing temperature and the longer the holding time at this temperature are, the larger is the spherulite size, because the memory effect of crystallinity is eliminated more thoroughly [25].

The crystal structure of PET has a triclinic unit cell. In the absence of nucleating agents and plasticizers, PET crystallizes slowly and consequently a rather fine dispersed crystal texture was obtained after cooling to room temperature [23, 26]. Compared with the wide

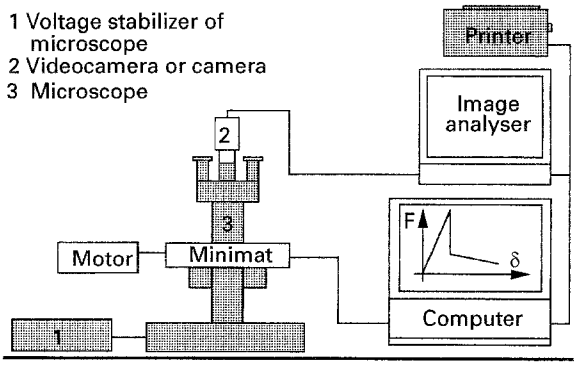

Figure 2 Schematic of testing fixture of Minimat unit on a microscope.

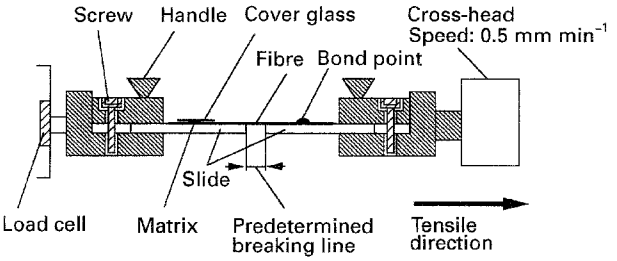

Figure 3 Schematic of tension appliance of Minimat with a fibre pull-out sample.

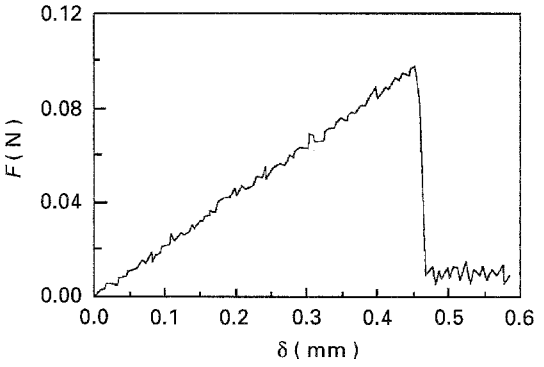

Figure 4 Typical load–displacement curve for a successful single fibre pull-out test.

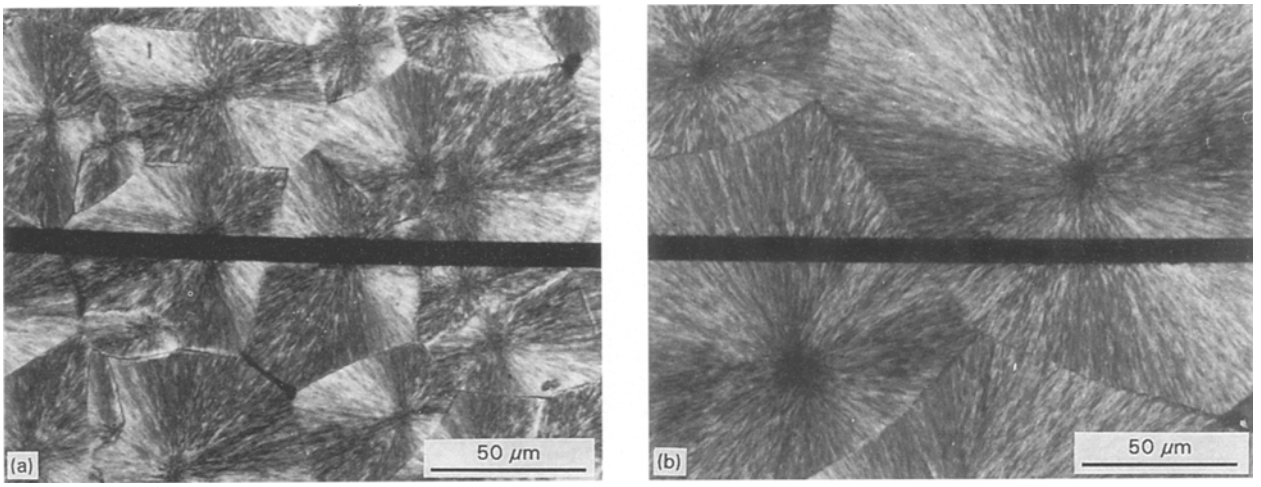

Figure 5 Processing-dependent PPS morphology around T700S fibre. Cooling rate (a) 20 °C min^{-1} and (b) 1 °C min^{-1}.

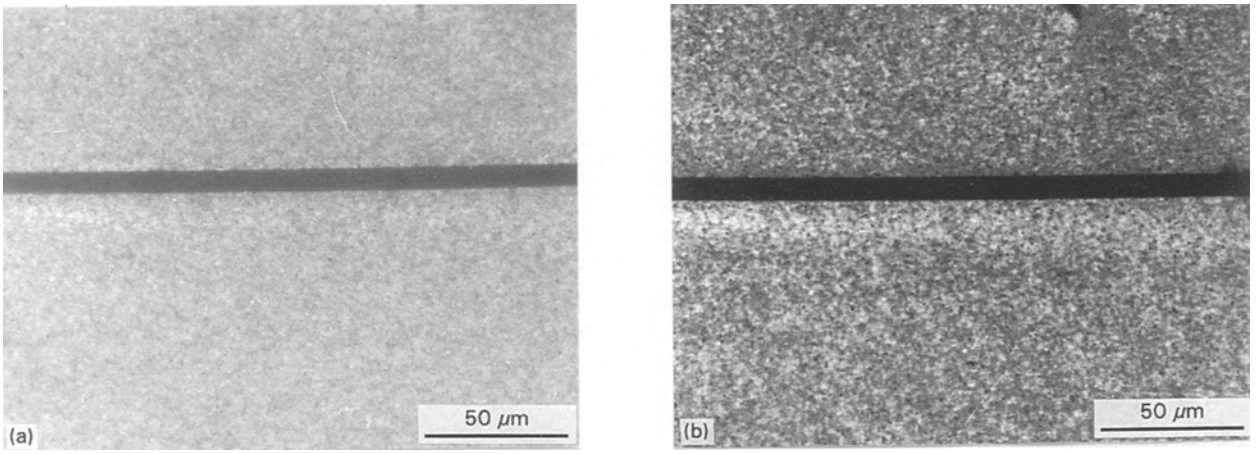

Figure 6 Processing-dependent PET morphology around T700S fibre. Cooling rate (a) 20 °C min^{-1} and (b) 5 °C min^{-1}.

spectrum of spherulite sizes achieved for the PPS system, the spherulite size of the PET polymer was almost insensitive to changes in the thermal processing history applied during sample manufacturing. It was also rather difficult to identify the spherulite boundaries. However, it was found that the slow cooling correlated with high crystallinity of the PET matrix [27].

Foreign particle/filler surfaces may play an important role in determining the microstructure of a semi-crystalline polymer. It was argued that the fibre–matrix interface plays an important role for the matrix morphology around the fibre [15–17, 28]. However, for the different cooling rates selected in this study, no recognizable change in the morphology caused by T700 fibre could be identified for the PPS and PET matrices, as shown in Figs 5 and 6. The matrix crystallization surrounding the carbon fibre took place in the same way as in the bulk polymer matrix.

Transcrystallinity can be achieved by melt shearing [29] or by isothermal crystallization [15]. It was indicated that for the CF/PPS systems a transcrystalline phase can be induced pulling the fibre to change the nucleation density on the fibre surface [30]. In this study, a transcrystalline layer was achieved combining both methods. The carbon fibre was touched, not pulled between 240–250 °C during cooling and afterwards the sample was isothermally crystallized for 10 min at 227 °C. Touching of the fibre was found to be sufficient to enhance the nucleation density on the fibre surface and to produce a transcrystalline layer, as shown in Fig. 7. The transcrystalline layer grew over the whole embedded fibre length, while the layer thickness varied. Transcrystallization occurred always before the bulk polymer crystallized. Reheating the

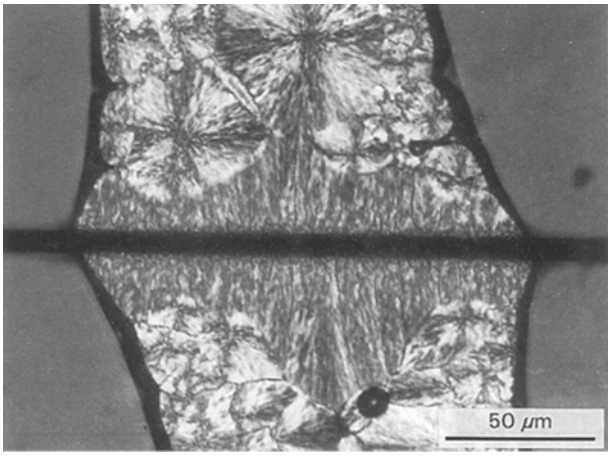

Figure 7 Typical PPS transcrystallization morphology around T700S fibre in fibre pull-out samples.

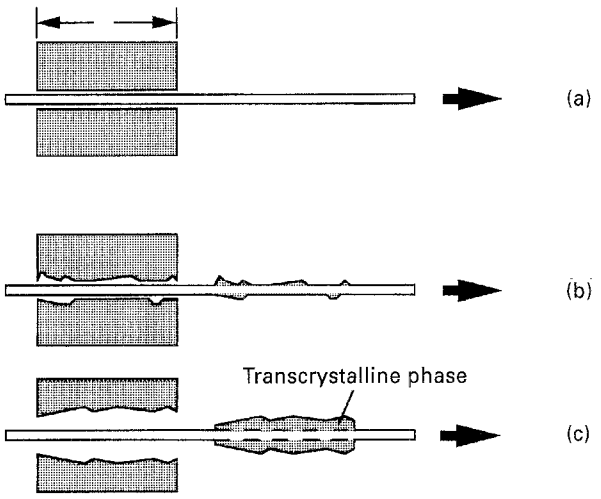

Figure 8 Schematics of typical failure paths of fibre pull-out in tests. (a) Interfacial failure; (b), (c), cohesive failure.

samples, the transcrystalline phase as well as the bulk crystalline spherulites became molten at the same temperature, T_m, so that a similar crystal structure in both areas can be assumed.

4.2. Failure mechanisms during fibre pull-out

In a fibre pull-out test, there are three possible failure modes [31–32]:

1. failure can occur when the maximum shear stress exceeds the interfacial shear strength;
2. yielding of the interphase is also possible, e.g. under conditions of a constant shear stress distribution along the embedded fibre length, as long as work-hardening effects are negligible;
3. if the energy release rate at the tip of an infinitesimal crack is greater than the crack growth resistance, i.e. the work of fracture per unit area of the interface, failure takes place by successive interfacial debonding.

It was observed from the experiments that the occurrence of fibre pull-out is sudden and catastrophic. This type of failure is more common to a brittle fracture rather than to a shear yielding failure. Since a shear stress concentration exists at the point where the fibre emerges from the matrix, this is the most likely point where the debonding probably starts and propagates rapidly along the interface (adhesive failure) or within the interphase (cohesive failure). From the load–displacement curves of the fibre pull-out tests for the PPS and PET systems (as shown in Fig. 4), a brittle failure cannot be excluded. The sudden decrease in the load suggests that some type of brittle fracture, rather than a yielding process, is involved. Unfortunately, it is not easy to distinguish the failure modes. Nevertheless, it can be stated that Equation 1 gives an indication of the interfacial bond strength between the fibre and matrix. After debonding, friction at the interface has to be overcome in order for the pull-out process to proceed. The frictional forces depend on the normal compressive stress acting from the matrix on to the fibre. Such a stress arises from resin shrinkage associated with the mismatch between coefficients of thermal expansion of the matrix and the reinforcing fibre [32]. The load–displacement curves for the PPS and PET systems show only a low friction load after debonding. One reason is probably due to a very small embedded fibre length. Upon reaching the critical load, the fibre is rapidly pulled out of the matrix so that the typical friction effect in the form of a slow decrease of force in the load–displacement curve was not observed [33].

During the fibre pull-out experiments, two basic fracture paths can be distinguished, as shown schematically in Fig. 8. The first one is the interfacial failure without recognizable damage of matrix or fibre, associated with no matrix coating the fibre surface after it was pulled-out; this is frequently referred to as an interfacial failure (Fig. 9). On account of a very strong fibre–matrix bond, failure occurred cohesively in the matrix. After the fibre was pulled out, the fibre surface was coated with a matrix layer (Fig. 10). In this cohesive failure path, the strength value calculated from Equation 1 indicates a combined contribution of interfacial bond strength and matrix strength. Another interesting cohesive failure path was observed for samples with a transcrystalline layer. The shear failure occurred along the boundaries between the transcrystalline phase and the bulk spherulites in the sample (Fig. 8(c)). However, failure

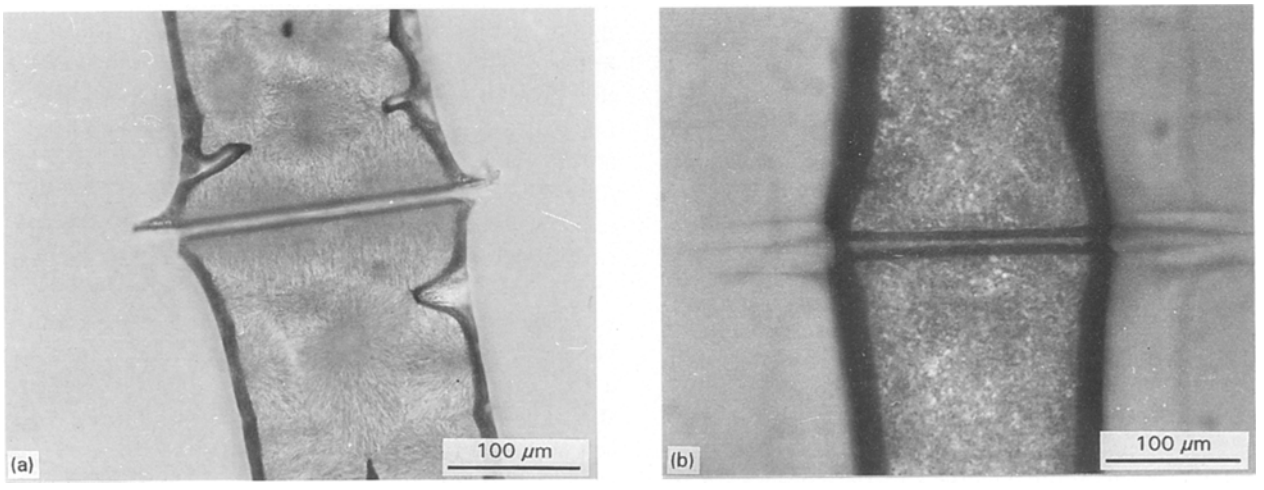

Figure 9 Interface failure of fibre pull-out in (a) T700/PPS and (b) T700/PET samples.

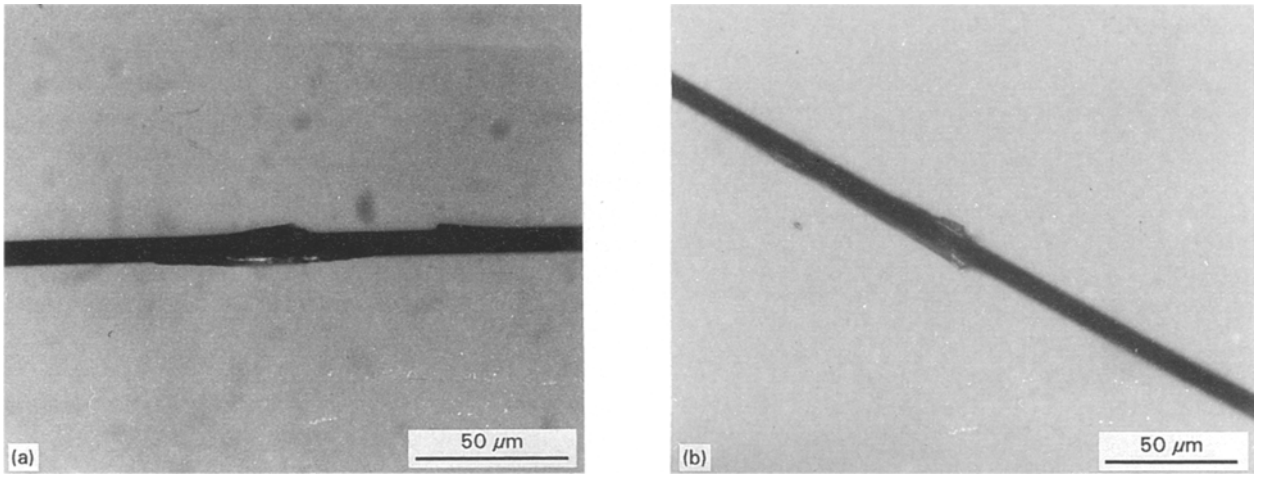

Figure 10 Cohesive failure of fibre pull-out in (a) T700/PPS and (b) T700/PET samples.

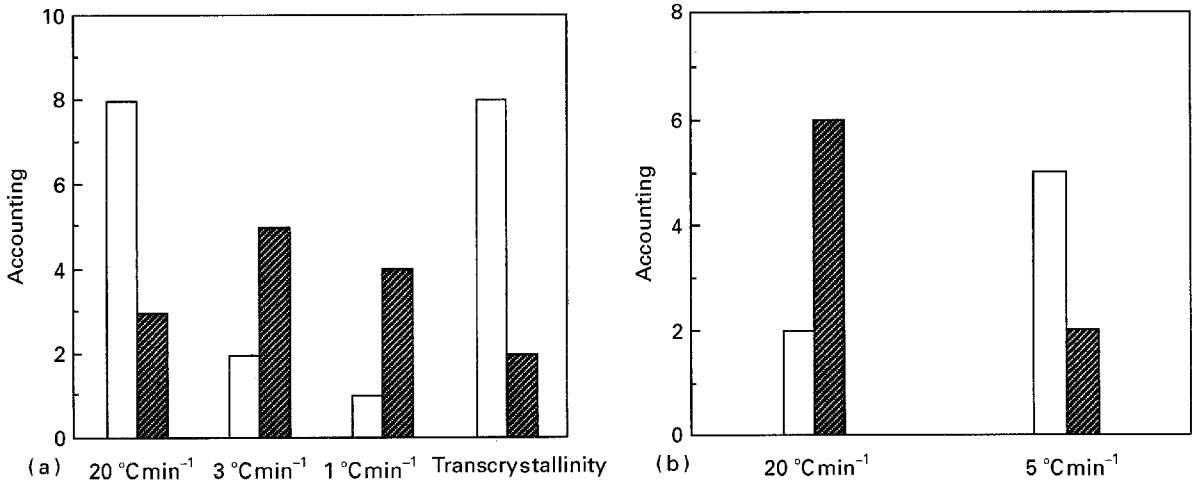

Figure 11 Frequency of two different failure paths in (a) T700/PPS and (b) T700/PET samples. □ Cohesive failure; ▨ interface failure.

in matrix close to the fibre surface was also observed, i.e. a failure path within the transcrystalline phase. Sometimes the cohesive failure path was observed only on one side of the fibre while the other side was a clear interfacial failure; this furthermore complicates the interpretation of the mechanical test results.

For the carbon fibre/PPS and carbon fibre/PET systems subjected to different processing histories, the total amount of specimens tested in each group and the accounting of two different failure paths are illustrated in Fig. 11. For the PPS system at a cooling rate of $20\,^{\circ}C\,min^{-1}$ almost three-quarters of the samples failed cohesively, while a change to interface failure was observed for the samples with lower cooling rates (Fig. 11(a)). For the transcrystalline samples, the weak boundaries between the transcrystalline phase around the fibre and the bulk spherulites is assumed to be relevant to the high frequency of cohesive failure. However, it is of interest to see that a different failure behaviour occurs for the carbon fibre/PET samples, compared to the PPS system. For the cooling rate of $20\,^{\circ}C\,min^{-1}$, six out of eight samples failed at the interface, while for $5\,^{\circ}C\,min^{-1}$ five out of seven samples failed cohesively, as shown in Fig. 11(b).

For the carbon fibre/PET as well as for the carbon fibre/PPS system, the average shear strength, τ_{ic}, calculated from Equation 1 for the cohesive failure path, was almost independent of the different cooling rates, even though calculations were made for the sample groups of different amounts of specimens. For the carbon fibre/PPS system the value was around 37 MPa while for carbon fibre/PET it amounted to 60 MPa (Fig. 12). This indicates that for the cohesive failure path the shear strength seems to be independent of processing conditions and matrix morphology. However, the average strength corresponding to the interface failure path is clearly dependent on the cooling rates and the resulting matrix morphology around the fibres. For low cooling rates and the transcrystalline morphology with the carbon fibre/PPS system, the shear strength corresponding to the interface failure path is higher than that associated with cohesive failure. It is of interest to note that for the carbon fibre/PPS system the interfacial failures mostly correlated with the higher values of shear strength while for carbon fibre/PET the cohesive failures lead to the best results. Due to the complicated failure mechanisms, it is, however, questionable to take the shear strength value corresponding to the cohesive failure path as a real measure of the fibre–matrix interfacial shear strength (if Equation 1 is used in the calculation). One can state, on the other hand, that this value gives at least the lowest margin of the apparent interfacial shear strength.

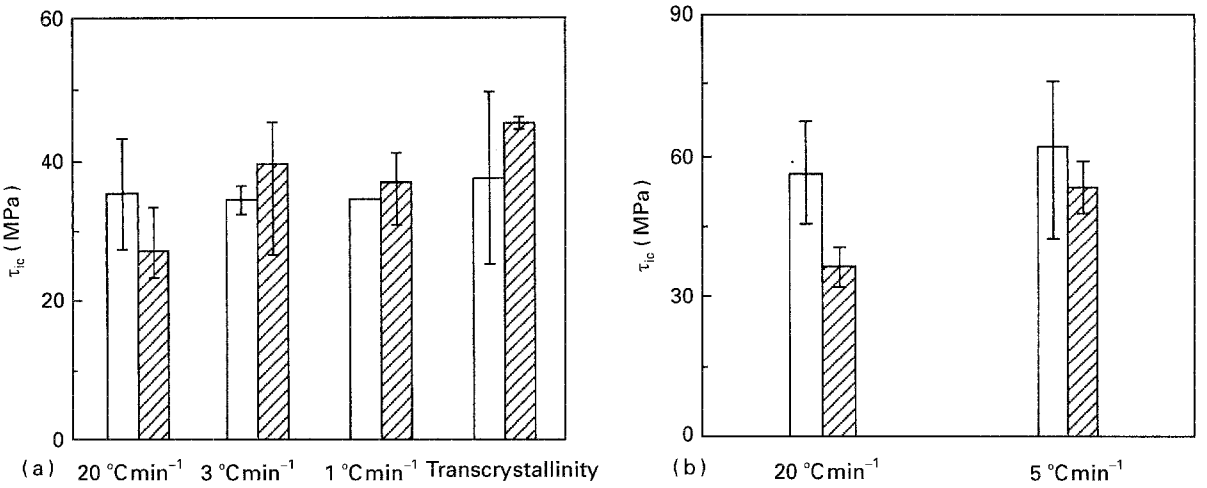

Figure 12 Average shear strength associated with cohesive and interface failure paths in (a) T700/PPS and (b) T700/PET samples. □ Cohesive; ▨ interface.

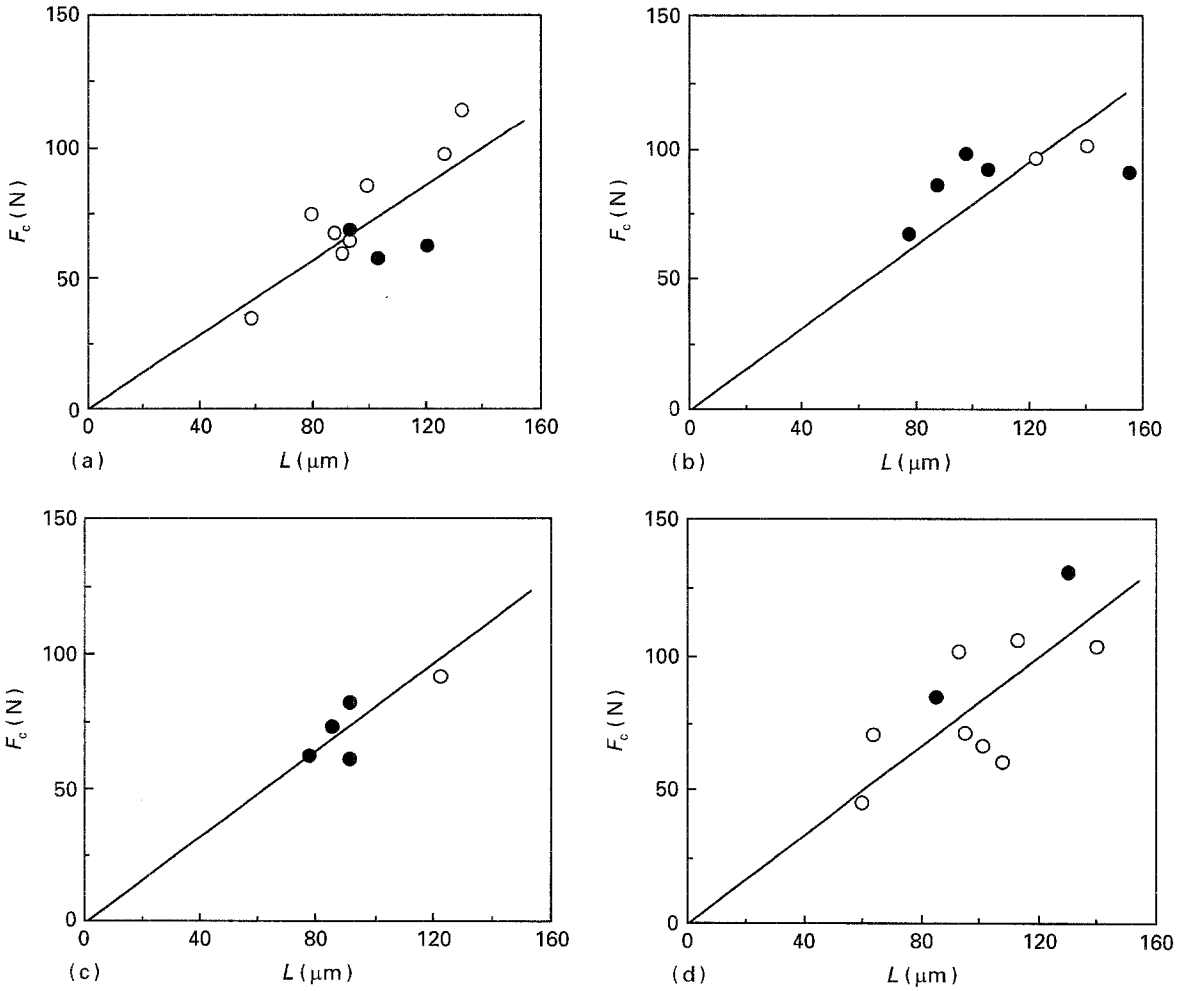

Figure 13 Critical pull-out loads versus embedded fibre length for T700/PPS samples. Cooling rate (a) 20 °C min^{-1}, (b) 3 °C min^{-1}, (c) 1 °C min^{-1} and (d) transcrystallinity. ● Interface; ○ cohesive.

4.3. Interfacial shear strength

When the interfacial shear strength is calculated with Equation 1, a linear relationship between the applied load versus the embedded fibre length is assumed, though a nonlinearity for the embedded fibre length, $L > 1$ mm, was observed [34]. In Figs 13 and 14, the relationships between the critical pull-out load and the embedded fibre length are illustrated for the T700/PPS and T700/PET samples subjected to the different processing conditions.

The average values of the interfacial shear strength obtained from the single fibre pull-out tests for the T700/PPS and T700/PET systems are summarized in Fig. 15. For the PPS system it can be seen that the interfacial shear strength increases as the cooling rate is reduced, although the difference was small if the

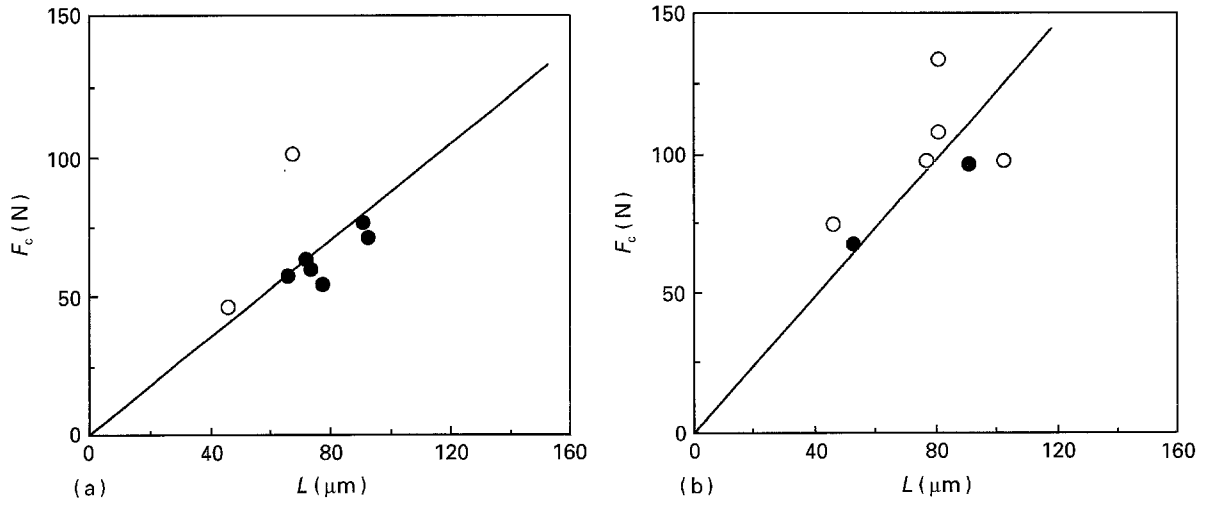

Figure 14 Critical pull-out loads versus embedded fibre length of T700/PET samples. Cooling rate (a) 1 °C min^{-1} and (b) 5 °C min^{-1}. ● Interface; ○ cohesive.

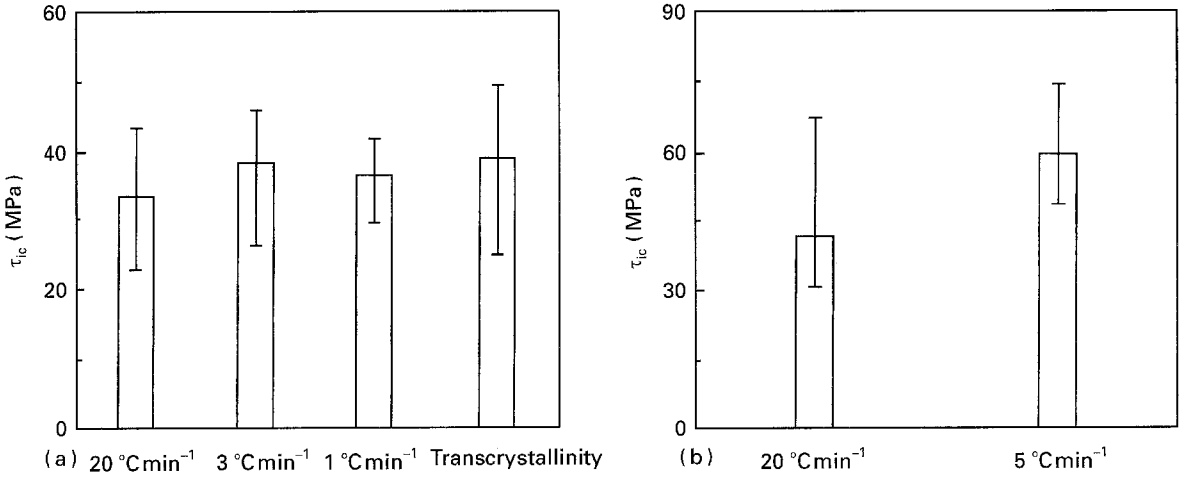

Figure 15 Interfacial shear strength versus processing histories of (a) T700/PPS and (b) T700/PET samples.

scatter of data is considered. Concerning the matrix morphology around the fibre, the slightly higher value of the interfacial shear strength correlated with larger spherulite size. A somewhat higher value was obtained for the samples with the transcrystalline phase, although it can be stated, in general, that the supermolecular microstructure did not improve the interfacial shear strength substantially.

There are many possible aspects associated with the interfacial shear strength, such as stress concentration and distribution, thermal and residual stresses, bonding between fibre and matrix, failure path, morphology and spherulite size, as well as microdefects etc. The level of the bond strength between a T700 carbon fibre and a PPS matrix can be considered to be poor. The highest average τ_i values were about 39 MPa, i.e. they achieved almost only half of the tensile strength (83 MPa) of the pure PPS [22]. It has been argued that the bonding between the untreated carbon fibre and the PPS polymer is intrinsically poor [35], which is consistent with the present results.

For the T700/PET system, only the cases of two different cooling rates 20 and 5 °C min^{-1} were investigated. Compared to the results of the PPS-based system, a clear increase of the interfacial shear strength for the T700/PET system was observed with decreasing cooling rate. For the cooling rate of 5 °C min^{-1}, the interfacial shear strength between T700 carbon fibre and the PET polymer reached almost 85% of the tensile strength (70 MPa) of the bulk PET [23]. This indicates an excellent adhesion between the fibre and matrix, while the values for the cooling rate of 20 °C min^{-1} were significantly lower, as shown in Fig. 15(b).

5. Conclusions

The effects of processing conditions and resulting matrix morphology on the interfacial bond strength of T700S/PPS and T700S/PET thermoplastic composites have been investigated using the single fibre pull-out experimental procedure. The processing temperatures and cooling histories of the single fibre pull-out samples were accurately controlled using a hot stage in order to produce different matrix morphologies around the fibre. The morphology of the PPS polymer was very sensitive to the cooling histories and a broad spectrum of spherulite sizes was obtained, while the morphology of the PET matrix was almost insensitive to the changes in the processing

conditions. It was observed that the T700 fibre has no clear influence on the surrounding PPS and PET matrix morphology, if direct cooling at a constant rate was selected. However, a transcrystalline PPS phase could be induced around the fibres if they were slightly moved (just by touching them) under isothermal crystallization conditions at 227 °C.

Fibre pull-out tests were conducted at room temperature. From the failure mechanisms, two basic failure paths were distinguished: debonding at fibre–matrix interface and cohesive failure in the matrix close to the fibre surface. These types of failure affect the evaluation and explanation of the interfacial shear strength between the fibre and the different matrices. If the global bond strength is concerned, one can state that a slow cooling rate and a resulting coarse spherulite morphology around the fibre correlated with a high interfacial shear strength. In the case of PPS a somewhat higher strength value was further obtained for samples with a transcrystalline phase around the fibre, however the improvement is not remarkable if the scatter of the experimental data is considered in the evaluation.

From a practical point of view, the argument for the advantages of thermoplastic composites is given in their potential for rapid, low-cost mass production. This potential cannot be reached if transcrystallization is aimed for as a tool for material improvement because the special processing histories need to be controlled accurately. Furthermore, a dramatic improvement in mechanical properties by transcrystallization is not clearly achievable as indicated by the results of this study.

Acknowledgements

Thanks are due to Toray Industries, Inc., Japan, Phillips Petroleum Singapore Chemicals Limited, and Toyobo Co., for supplying the testing materials. Dr L. Ye expresses appreciation to the Australian Research Council (ARC) for supporting this study by a research grant (AB-9332172). Professor K. Friedrich addresses his thanks to the Fonds Der Chemischen Industrie, Frankfurt, Germany for help with his research activities in 1995.

References

1. J. DENAULT and T. VU-KHANH, *Polym. Compos.* **13** (1992) 361.
2. W. I. LEE, M. F. TALBOTT, G. S. SPRINGER and L. A. BERGLUND, *J. Reinforced Plast. Compos.* **6** (1987) 2.
3. M. F. TALBOTT, G. S. SPRINGER and L. A. BERGLUND, *J. Compos. Mater.* **21** (1987) 1057.
4. P. CEBE, S. D. HONG, S. CHUNG and A. GUPTA, in Toughened composites, ASTM STP-937, edited by N. J. Johnston (ASTM, Philadelphia, 1987) p. 342.
5. W. J. CANTWELL, P. DAVIES and H. H. KAUSCH, *Compos. Struct.* **14** (1990) 151.
6. P. VAUTEY, *SAMPE Quart.* **21** (1990) 23.
7. L. YE and K. FRIEDRICH, *Compos. Sci. Tech.* **46** (1993) 187.
8. F. N. COGSWELL, in 28th SAMPE Symposium (SAMPE, 1983) p. 528.
9. J. A. PEACOCK, B. FIFE, E. NIELD and C. Y. BARLOW, in Composite interfaces, edited by H. Ishida and J. L. Koenig (Elsevier, New York, 1986) p. 143.
10. M. J. FOLKES and S. T. HARDWICK, *J. Mater. Sci. Lett.* **6** (1987) 656.
11. *Idem., J. Mater. Sci.* **25** (1990) 2598.
12. M. G. HUSON and W. J. MCGILL, *J. Polym. Sci., Phys.* **23** (1985) 121.
13. HAGENSON et al., 34th SAMPE Symposium, **2** (1989) 2255.
14. M. J. FOLKES, S. T. HARDWICK and W. K. WONG, in Polymer composites, edited by B. Sedlacek (W. de Gruyter & Co, Berlin, 1986) p. 33.
15. J. L. THOMASON and A. A. VAN ROOYEN, *J. Mater. Sci.* **27** (1992) 889.
16. B. MANASSE, *Ibid.* **27** (1992) 6047.
17. J. H. E. CHEN and B. S. HSIAO, *Polym. Eng. Sci.* **32** (1992) 280.
18. L. T. DRZAL and M. MADHUKAR, *J. Mater. Sci.* **27** (1993) 569.
19. S. MERETZ, W. AUERSCH, C. MAROTZKE, E. SCHULZ and A. HAMPE, *Compos. Sci. Tech.* **48** (1993) 285.
20. H. KOBAYASHI, E. HAYAKAWA, T. KIKUTANI and A. TAKAKU, *Adv. Composite. Mater.* **1** (1991) 155.
21. Carbon fibres, Material Information, Toray Industries, Inc., Tokyo 103, Japan (1992).
22. P. G. GALANTY and J. J. RICHARDSON, in Engineering materials handbook Vol. 2–Engineering plastics (ASM International Metals Park, OH, 1988) p. 172.
23. D. G. BRADY, *Ibid.* p. 186.
24. P. MARSHALL and J. PRICE, *Composites* **22** (1991) 335.
25. J. M. SCHULTZ, in Thermoplastic composite materials, edited by L. A. Carlsson, Vol. 7, series editor R. B. Pipes (Elsevier Science Publisher BV, Amsterdam, 1991), p. 31.
26. V. E. REINSCH and L. REBENFELD, *Polym. Compos.* **13** (1992) 353.
27. L. YE and K. FRIEDRICH, *Composites* **24** (1993) 557.
28. P. H. I. BUSSI, *J. Mater. Sci.* **26** (1991) 6373.
29. J. L. THOMASON and A. A. VAN ROOYEN, *Ibid.* **27** (1992) 897.
30. L. LOPEZ and G. L. WILKER, *J. Thermoplast. Compos. Mater.* **4** (1991) 58.
31. M. R. PIGOTT, *Compos. Sci. Technol.* **30** (1987) 295.
32. P. J. HERRERA-FRANCO and L. T. DRZAL, *Composites* **23** (1992) 2.
33. T. J. MACKIN, J. YANG and P. D. WARREN, *J. Am. Ceram. Soc.* **75** (1992) 3358.
34. M. R. PIGOTT, in Composite applications: the role of matrix, fibre and interface, edited by T. I. Vigo and B. J. Kinzig (VCH Publishers, New York, 1992) p. 221.
35. C. T. SPAMER and N. D. BRINK, 33rd SAMPE Symposium (SAMPE, 1988) p. 284.

Received 23 January 1995
and accepted 22 March 1995